Human Pathology (2019) **90**, 60–69

ELSEVIER

Human PATHOLOGY

www.elsevier.com/locate/humpath

Original contribution

Recurrent PDL1 expression and *PDL1* (*CD274*) copy number alterations in breast implant–associated anaplastic large cell lymphomas☆,☆☆

Valentina Tabanelli MD[a,*], Chiara Corsini BS[b], Stefano Fiori MD[a], Claudio Agostinelli MD, PhD[c], Angelica Calleri BS, PhD[a], Stefania Orecchioni BS, PhD[b], Federica Melle BS, PhD[a], Giovanna Motta BS, PhD[a], Anna Rotili MD[d], Arianna Di Napoli MD, PhD[e,1], Stefano A. Pileri MD, PhD[a,1]

[a]*Division of Diagnostic Haematopathology, European Institute of Oncology, IRCCS, Milan 20141, Italy*
[b]*Laboratory of Hematology-Oncology, European Institute of Oncology, IRCCS, Milan 20141, Italy*
[c]*Section of Haematopathology, Institute of Haematology & Clinical Oncology 'L&A Seragnoli,' S.Orsola-Malpighi Hospital, Bologna 40138, Italy*
[d]*Division of Breast Radiology, European Institute of Oncology,IRCCS, Milan 20141, Italy*
[e]*Pathology Unit, Department of Clinical and Molecular Medicine, Sapienza University of Rome, Sant'Andrea Hospital, Rome 00189, Italy*

Received 10 February 2019; revised 8 May 2019; accepted 8 May 2019

Keywords:
Breast implant;
Anaplastic lymphoma;
PDL1;
Copy gain;
Polysomy

Summary Breast implant–associated anaplastic large cell lymphoma (BI-ALCL) is a variant of anaplastic large cell lymphoma arising within seroma effusion associated with breast implants. BI-ALCL is a rare disease, recently recognized as a new provisional entity by the 2017 revised World Health Organization classification. All BI-ALCLs tested so far showed a "triple-negative" genetic profile—negative for *ALK, DUSP22,* and *TP63* rearrangements—and were characterized by mutational and gene expression profiles consistent with aberrant activation of the JAK/STAT pathway. The active form of STAT3 (pSTAT3) is constantly expressed in BI-ALCLs and may favor tumor immune escape by triggering the transcription of *PDL1* (*CD274*), a gene encoding the immune-checkpoint molecule programmed cell death ligand 1 (PDL1); immunohistochemical positivity for PDL1 has been recently described in 3 BI-ALCL cases, and one of them also harbored *PDL1* gene amplification. We evaluated PDL1 and pSTAT expression by immunohistochemistry and *PDL1* copy number alterations (CNAs) at chromosome 9p24.1 by fluorescent in situ hybridization in a cohort of 9 BI-ALCL cases; we also investigated the presence of tumor-infiltrating programmed cell death 1 (PD1)+ T cells (tumor-infiltrating lymphocytes, or TILs) and PDL1+ tumor-associated macrophages (TAMs) in BI-ALCL microenvironment. Tumor cells expressed PDL1 in 5 (56%) of 9 cases and harbored *PDL1* CNAs in 3 (33%) of 9 cases; immunohistochemistry for pSTAT3 was positive in all 6 cases tested (100%), indicative of active JAK/STAT signaling. We observed *PDL1* CNAs only among PDL1-positive cases, whereas PD1+

☆ Competing interest: S. A. P. received honoraria for educational activities from Celgene. The remaining authors have no financial relationship to disclose.
☆☆ Funding/Support: This work was supported by the 5x1000 Grant No. 21198 from the Italian Association for Cancer Research, Milan.
* Corresponding author at: Division of Diagnostic Haematopathology, European Institute of Oncology, IRCCS, via Ripamonti 435, 20141 Milan, Italy.
E-mail address: valentina.tabanelli@ieo.it (V. Tabanelli).
[1] A. D. N and S. A. P. contributed equally to this work.

https://doi.org/10.1016/j.humpath.2019.05.007

TILs and PDL1+ TAMs were present at variable levels in both PDL1-positive and PDL1-negative BI-ALCLs. We report frequent PDL1 expression and recurrent *PDL1* CNAs in BI-ALCLs: our data suggest that 9p24.1 alterations represent a common mechanism of PDL1 overexpression in this disease, likely acting in synergy with constitutive pSTAT3 signaling. In PDL1-positive cases without chromosomal aberration, PDL1 expression may be induced by JAK/STAT signaling alone and/or others alternative pathways. BI-ALCL microenvironment hosts variable amounts of PD1+ TILs and PDL1+ TAMs, suggesting the presence of an active PD1/PDL1 axis. These findings may be of therapeutic value in advanced-stage patients who may benefit from a PD1/PDL1 blocking treatment.

1. Introduction

The revised World Health Organization classification of lymphoid tumors recognizes breast implant–associated anaplastic large cell lymphoma (BI-ALCL) as a new provisional entity for its unique features: it is a rare ALCL variant arising in the effusion and/or the capsule surrounding saline or silicon-filled breast implants [1]. BI-ALCL usually has a favorable outcome, being confined to the periprosthetic effusion and thus cured by surgery alone. However, the minority of cases that develop extraprosthetic involvement display an aggressive clinical course, at times leading to death from disease [2,3].

Genomic studies on BI-ALCL biology have been limited by the rarity of this disease: a recent meta-analysis estimates an annual incidence of less than 5 cases per 100 000 women with implants [4].

From a genetic perspective, BI-ALCL shows a so-called "triple-negative" profile: it characteristically lacks *ALK* rearrangements, and all cases tested so far have been consistently negative for *DUSP22* and *TP63* rearrangements (2 mutually exclusive chromosomal abnormalities recurrently detected in systemic and cutaneous ALK-negative ALCL) [3,5].

Aberrant activation of STAT3 seems to be a key player in BI-ALCL oncogenesis: neoplastic cells nearly always express phosphorylated STAT3 Y705 (pSTAT3) by immunohistochemistry, in contrast to the variable positivity observed in other ALK-negative ALCLs [3,5]. Although in ALK-positive ALCL the chimeric ALK protein drives STAT3 phosphorylation [6], in BI-ALCL, pSTAT3 overexpression can be caused, at least in part, by mutational events in genes involved in the JAK/STAT pathway: roughly one-third of the cases bear activating mutations of genes involved in the JAK/STAT pathway (*STAT3, JAK1, JAK3)* or loss-of-function mutation of *SOCS1*, a negative regulator of JAK kinase activity [3,5,7-10]. However, because pSTAT3 is uniformly positive regardless of the mutational status, alternative genetic mechanisms may be involved in JAK/STAT pathway activation.

Several investigators have also proposed a role for chronic antigen stimulation and immune escape mechanisms in BI-ALCL pathogenesis: silicone degradation products and biofilm organisms on the implant surface may stimulate and maintain T-cell activation [11,12], whereas BI-ALCL–derived cell lines can release immunosuppressive cytokines fostering a tumor-tolerant microenvironment [13,14].

Persistent JAK/STAT signaling may also favor an immunosuppressive tumor microenvironment in BI-ALCL: pSTAT3 enhances the transcription of the immune-checkpoint molecule PDL1 (encoded by *PDL1/CD274*) [15,16] that engages the programmed cell death 1 (PD1) receptor on tumor-infiltrating T cells (tumor-infiltrating lymphocytes, or TILs), promoting reversible T-cell exhaustion [17]. PDL1 immunohistochemical expression has been recently reported in 3 BI-ALCL cases, and one of them also harbored *PDL1* gene amplification [18,19].

Because PD1/PDL1 blockade may represent a therapeutic strategy—especially for patients with aggressive or recurrent disease—we investigated PDL1 and pSTAT3 expression by immunohistochemistry in a cohort of 9 BI-ALCL cases. Besides pSTAT3-mediated transcriptional upregulation, PDL1 expression can also be boosted by increased gene dosage due to *PDL1* copy number alterations (CNAs), so we also evaluated *PDL1* genetic abnormalities at chromosome 9p24.1 by fluorescence in situ hybridization (FISH). Finally, to further investigate the PD1/PDL1 axis in BI-ALCL microenvironment, we examined PD1 and PDL1 expression in TILs and tumor-associated macrophages (TAMs), respectively.

2. Materials and methods

2.1. Patients and specimens

Formalin-fixed, paraffin-embedded archival specimens from 9 patients with BI-ALCL at first presentation were collected in accordance with local institutional review board protocols. Cases were reviewed and diagnosed according to 2017 revised World Health Organization classification [1] by 4 expert hematopathologists (V. T., S. F., A. D. N., and S. A. P.). The disease was staged using the TNM staging system proposed by Clemens et al [2].

2.2. Immunohistochemistry

Immunohistochemistry was performed on 2-μm-thick formalin-fixed, paraffin-embedded whole tumor sections using

a Dako Autostainer Link48 (Dako Agilent, Glostrup, Denmark), after antigen retrieval (PTLink at 92°C for 5 minutes in Dako EnVision Flex Target Retrival Solution High pH). The primary antibodies used were PDL1 (clone E1L3N, 1:200; Cell Signalling, Danvers, Massachusetts), pSTAT3 (clone D3A7, 1:100; Cell Signaling), PD1 (clone NAT105, 1:4; Abcam, Cambrige, UK), and CD3 (clone SP7, 1:100; BioOptica, Milan, Italy). Slides were developed using fast red (alkaline phosphatase-chromogen) or with 3,3′-diaminobenzidine chromogen (Dako) after peroxidase block for 5 minutes, counterstained with hematoxylin, dehydrated, and coverslipped.

For PDL1, both cytoplasmic and cell-membrane staining patterns were recorded. PDL1 expression was scored with a semiquantitative approach (H-score: range, 0-300) multiplying the percentage of positive malignant cells (0%-100%) and the average intensity of staining (0, no staining; 1+, weak staining; 2+, moderate staining; 3+, strong staining). Samples were considered positive for pSTAT3 when ≥20% of neoplastic cells showed nuclear staining, as previously described [20]. Endothelial cells and macrophages were used as internal positive controls for pSTAT3 and PDL1 staining, respectively. Microphotographs of BI-ALCL1 to BI-ALCL6 were taken using an Olympus, Tokyo, Japan BX53 light microscope with an Olympus DP71 camera. Original magnifications are specified in figure legends.

2.3. Fluorescence in situ hybridization

FISH was performed on 4-μm-thick sections with Texas Red CD274 (PDL1)–labeled probe and FITC CEN9q–labeled centromeric probe as an internal control, according to the manufacturer's recommendations (Abnova, Taipei City, Taiwan). Because BI-ALCL cells often formed small clusters within a fibrinoid material, FISH evaluation was focused on areas with the highest density of neoplastic cells, previously highlighted on hematoxylin and eosin–stained slides. Approximately 100 cells per case were analyzed; nuclei without CEN9q signals and overlapping nuclei were excluded from the count.

Cutoff value was determined by analyzing 10 reactive lymph nodes as normal controls. The ratio of *PDL1* (red) signals to centromere 9 (green) signals was evaluated in 200 nuclei: the mean ratio + 3 SDs (corresponding to the value of 1.23) was assumed as the upper cutoff for copy gain and amplification. CNAs were further classified according by Roemer et al [21]: nuclei were defined as amplified if the target/control probe ratio was ≥3:1, as copy gain if the probe ratio was >1:1 but <3:1, or as polysomic for chromosome 9 if the probe ratio was 1:1, but more than 2 copies of each probe were detected. The MDA-MB-436 triple-negative breast cancer cell line, known to harbor *PDL1* amplification (Cancer Cell Line Encyclopedia, www.broadinstitute.org/ccle), was used as a positive control: MDA-MB-436 cells were purchased from the American Type Culture Collection (Manassas, VA), tested and authenticated by Stem cell Elite ID (Promega, Madison, US), and cultured as previously described [22]. MDA-MB-436 cells from culture were centrifuged, fixed in 10% neutral-buffered formalin, suspended in agar, and embedded in paraffin blocks. FISH analysis of cell blocks confirmed *PDL1* amplification in MDA-MB-436 cell nuclei (Supplementary Fig. S1).

BI-ALCL cases were classified by the highest observed level of 9p24.1 alteration. The spectrum of 9p24.1 CNAs (amplification, copy gain, polysomy) and residual disomy (normal 9p24.1 copy numbers) was quantified in each case (Table 1). Images were taken using an Olympus BX51 fluorescence microscope and Olympus cellSens image acquisition software.

2.4. Assessment of CD3, PD1, and PDL1 in tumor microenvironment

PD1 and CD3 expression in TILs was quantified in 6 periprosthetic capsule specimens by 2 hematopathologists (V. T. and S. F.); discrepancies in scoring (<10% of cases) were discussed by the third pathologist until consensus was reached. The samples were analyzed with the objective lens of 40×/0.75 Olympus UPlanFL (Olympus), corresponding to an area of 0.237 mm^2. PD1- and CD3-positive lymphocytes were counted in 5 high-power fields (HPFs) along the inner edge of the capsule and scored as the average number of positive

Table 1 Spectrum of *PDL1* genetic alterations in BI-ALCLs

Case ID	Cytogenetics							
	PDL1 IHC	No. of tumor cells	Disomy (% cells)	Polysomy (% cells)	No. of signals	Copy gain (% cells)	No. of signals	Amplification (% cells)
BI-ALCL 1	+	103	12	65	3-6	23	3-8R:2G	–
BI-ALCL 2	+	102	10	90	3-6	–	–	–
BI-ALCL 3	+	108	44	56	3	–	–	–
BI-ALCL 4	–	95	100	–	–	–	–	–
BI-ALCL 5	–	98	100	–	–	–	–	–
BI-ALCL 6	–	109	100	–	–	–	–	–
BI-ALCL 7	+	102	100	–	–	–	–	–
BI-ALCL 8	+	NE	NE	NE	NE	NE	NE	NE
BI-ALCL 9	–	110	100	–	–	–	–	–

Abbreviations: G, CEN9q FITC green signal; NE, not evaluable due to technical pitfalls; R, *PDL1* (*CD274*) Texas red signal.

Table 2 Clinical, pathological, and genetic features of BI-ALCL cases

Case ID	Age at diagnosis (y)	Interval to BI-ALCL (y)	Reason for implant	Type of implant	Clinical presentation	TNM (stage) [a]	Immunophenotype [b]	PDL1 IHC (H-score)	*PDL1* FISH	pSTAT3 IHC [c]
BI-ALCL 1	71	4	Breast cancer reconstruction	Macrotextured, silicone gel filled	Right-side effusion	T1N0M0 (IA)	CD30+, TIA1+, CD3–, CD4–, CD8–, EMA+/–, ALKc–, PAX5–	Positive (200)	Copy gain	Positive (90)
BI-ALCL 2	32	5	Breast cancer reconstruction	Macrotextured, silicone gel filled	Right-side effusion	T1N0M0 (IA)	CD30+, TIA1+, perforin–, CD3+, CD2-, CD5+, CD7+, CD4+, CD8–, EMA+, ALKc–, PAX5–	Positive (300)	Polysomy	Positive (30)
BI-ALCL 3	69	7	Breast cancer reconstruction	Macrotextured, silicone gel filled	Right-side effusion	T1N0M0 (IA)	CD30+, TIA1+, perforin+, CD3+, CD2+, CD5+, CD7–, CD4+, CD8–, ALKc–, PAX5–	Positive (250)	Polysomy	Positive (80)
BI-ALCL 4	60	5	Breast cancer reconstruction	Macrotextured, silicone gel filled	Right-side effusion	T1N0M0 (IA)	CD30+, TIA1+, perforin+/–, CD3+, CD4+, CD8–, EMA+, ALKc–, PAX5–, CD20–	Negative (0)	Disomy	Positive (80)
BI-ALCL 5	52	7	Breast cancer reconstruction	Macrotextured, silicone gel filled	Right-side effusion and thickening of periprosthetic capsule	T1N0M0 (IA)	CD30+, TIA1+, perforin–, CD3–, CD2-, CD5–, CD7–, CD4+, CD8–, EMA–/+, ALKc–, PAX5–	Negative (0)	Disomy	Positive (70)
BI-ALCL 6	38	11	Cosmetic	Macrotextured, silicone gel filled	Right-side effusion	T1N0M0 (IA)	CD30+, TIA1+/–, perforin+/–, CD4+/–, CD8–, EMA–/+, ALKc–	Negative (0)	Disomy	Positive (30)
BI-ALCL 7	49	6	Breast cancer reconstruction	Macrotextured, silicone gel filled	Left-side effusion and contralateral lymph nodes enlargement	T1N1M0 (IIB)	CD30+, ALK–, CD8–, GrB+/–, CD4+, CD3–, CD15+/–, MUM1+, CD25+, PD1-, ALKc–, PAX5–	Positive (300)	Disomy	ND
BI-ALCL 8	51	21	Cosmetic	Macrotextured, silicone gel filled	Right-side effusion and lymph nodes enlargement	T4N1M0 (III)	CD30+, CD3–, CD4+/–, CD25+, CD8–, GrB–, ALKc–, CD20–	Positive (70)	NA	ND
BI-ALCL 9	49	7	Cosmetic	Macrotextured, silicone gel filled	Left-side mass	T4N0M0 (IIA)	CD30+, CD15+, GrB+, CD3–, CD4+, CD8–, ALKc–, PAX5–, CD79a+	Negative (0)	Disomy	ND

Abbreviations: EMA, epithelial membrane antigen; GrB, granzyme B; IHC, immunohistochemistry; ND, not done; NE, not evaluable; TIA1, T-cell intracellular antigen-1.

[a] Based on the TNM staging system proposed by Clemens et al [2].

[b] (+) positive, >75% tumor cells staining; (+/–) 50% to 75% tumor cells staining; (–/+) 25% to 49%; (–) negative, 0% tumor cells staining.

[c] Percentage of tumor cells with nuclear staining. Positivity cutoff: ≥20% nuclear staining.

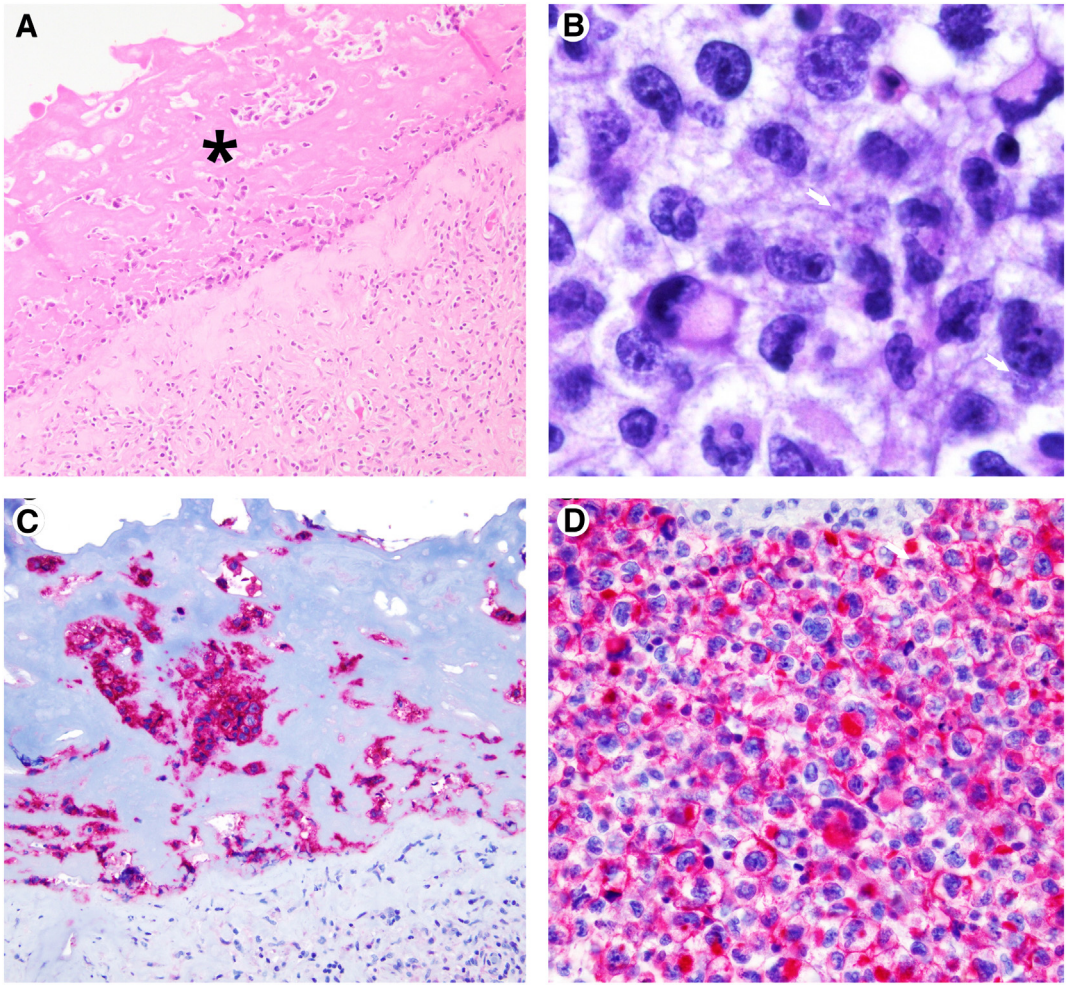

Figure 1 Morphologic and immunophenotypic findings in BI-ALCL. A, Low-power hematoxylin and eosin stain from BI-ALCL 2 shows neoplastic cells suspended in a fibrinoid material lining the inner surface of the capsule (*; original magnification ×100). B, High-power hematoxylin and eosin stain from BI-ALCL 3 highlights large pleomorphic cells surrounded by a clear halo admixed with scattered hallmark cells with horseshoe- or kidney-shaped nuclei (original magnification ×600). C and D, CD30 immunohistochemical staining is strongly positive in both specimens (original magnifications ×100 and ×400).

TILs per HPF. TAMs expressing PDL1 were also recorded as average number per HPF.

3. Results

3.1. Cohort characteristics

Clinical data are summarized in Table 2. All patients were women, with a median age of 51 years (range, 32-71 years); the median interval from implant placement to BI-ALCL presentation was 7 years (range, 4-21 years). Six (67%) of 9 patients presented with effusion-limited BI-ALCL, whereas the remaining 3 patients (33%) showed extracapsular disease: one had effusion and nodal involvement, one presented with breast mass, and the last one had breast mass and lymph node involvement. All patients underwent bilateral removal of the implants; patients with extracapsular disease also received cyclophosphamide, doxorubicin, vincristine, and prednisone

Figure 2 Analyses of the *PDL1* locus, PDL1, and pSTAT3 immunohistochemical expression in BI-ALCL. Representative images of cases with *PDL1* CNAs by FISH (original magnification ×1000). A, BI-ALCL 1 cells display both *PDL1* copy gain (5 copies of *PDL1* [red] compared with 2 CEN9q centromeric probes [green]), polysomy associated with relative copy gain by FISH (arrow: 5 copies of *PDL1* and 3 CEN9q probes), or residual disomy (arrowhead: 2 copies of *PDL1* and 3 CEN9q each). D, BI-ALCL 2 and BI-ALCL 3 show *PDL1* polysomy: BI-ALCL 2 harbors cells with 4, 5, and 6 copies of *PDL1* and CEN9q each;. G, BI-ALCL 3 presents cells with 3 copies of *PDL1* and CEN9q each. J, BI-ALCL 4 is disomic for 9p24.1, carrying 2 copies *PDL1* and CEN9q. PDL1 and pSTAT3 expression by immunohistochemistry in the same cases (original magnification ×400): positive PDL1 staining is present in BI-ALCL 1 (B), BI-ALCL 2 (E), and BI-ALCL 3 (H), whereas it is absent BI-ALCL 4 (K). C, F, I, and L, All cases are positive for pSTAT3 staining.

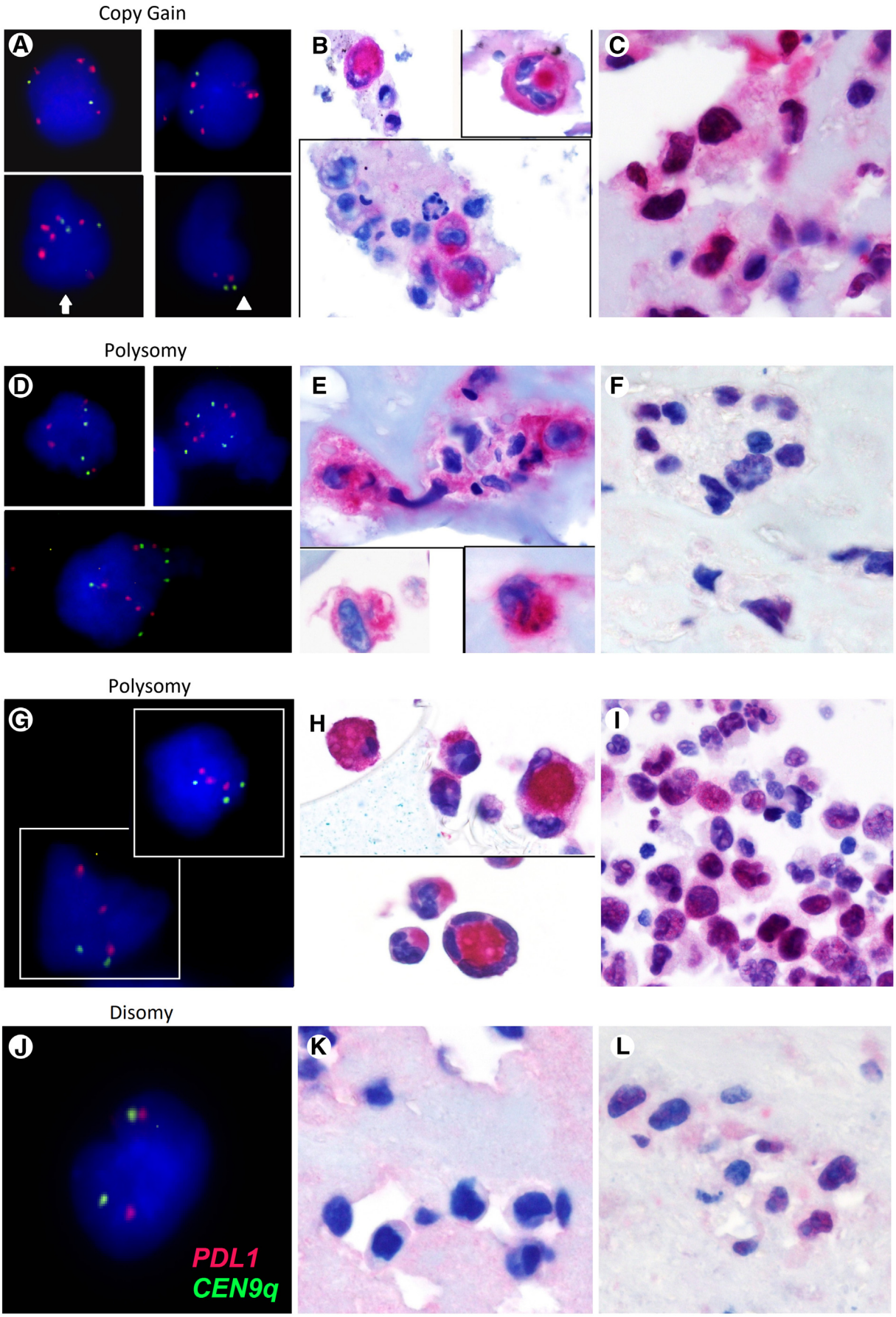
Copy Gain
A
B
C
Polysomy
D
E
F
Polysomy
G
H
I
Disomy
J
K
L
PDL1
CEN9q

chemotherapy or cyclophosphamide, doxorubicin, vincristine, etoposide, and prednisone chemotherapy.

3.2. Histopathologic features

Effusion-limited BI-ALCL specimens presented similar morphologic features: small clusters of tumor cells floated within serous/fibrinoid material or were confined to the inner surface of the capsule surrounding the implant (Fig. 1A); neoplastic cells were large with pleomorphic, multilobated, kidney-shaped nuclei and abundant eosinophilic cytoplasm (Fig. 1B). Patients with extracapsular disease presented with cohesive sheets of tumor cells that diffusely infiltrated the capsule and/or the pericapsular tissues, with necrotic areas. In cases with lymph node involvement, neoplastic cells invaded the nodal parenchyma with a nodular and/or a sinusoidal cohesive pattern.

CD30 was strongly positive in all cases (Fig. 1C and D), whereas ALK protein was always negative. BI-ALCL cases showed incomplete T-cell phenotype with expression of at least one of the tested cytotoxic markers (Tia1, perforin, granzyme B). Additional phenotypic data are shown in Table 2.

3.3. PDL1 expression and PDL1 CNAs in BI-ALCL tumor cells

PDL1 positivity was frequently observed in BI-ALCL (Table 2 and Fig. 2): 5 (56%) of 9 cases expressed PDL1 with a median H-score of 250 (range, 70-300); PDL1 was positive in 3 (50%) of 6 effusion limited cases and in 2 (67%) of 3 cases with extracapsular disease and/or lymph node involvement (Fig. 3). Tumor cells were positive for nuclear pSTAT3 at a variable level (with immunostaining in 30% to 100% of tumor cell nuclei) in all 6 cases tested (100%) (Table 2 and Fig. 2).

Fluorescent in situ hybridization analysis was successful in 8 (89%) of 9 cases; we found 9p24.1 CNAs in 3 cases (33%), as depicted in Fig. 2: 1 case showed *PDL1* relative copy gain and 2 had polysomy of 9p; all 3 cases with 9p24.1 CNAs were effusion-limited BI-ALCL. The remaining 5 cases were disomic for 9p24.1. No one case showed *PDL1* amplification. In copy gain and polysomic samples, we also detected neoplastic cells with lower-level 9p24.1 CNAs and/or residual disomic cells. More specifically, sample BI-ALCL1 presented *PDL1* copy gain in 23% of cells, 9p polysomy in 65% cells, and residual disomy in 12% of cells; polysomic samples BI-ALCL2 and BI-ALCL3 also harbored 10% and 44% residual disomic cells, respectively (Table 1); this pattern resembles the spectrum of 9p24.1 alterations described by Roemer et al [21] in classical Hodgkin lymphomas.

Among the 5 cases with positive PDL1 staining, 3 (60%) harbored *PDL1* CNAs and 1 (20%) was disomic for 9p24.1, and in the other one (20%), FISH was not analyzable because of technical artifacts; PDL1-negative cases were consistently negative for *PDL1* CNAs.

3.4. Assessment of CD3, PD1, and PDL1 expression in BI-ALCL microenvironment

The specimens relative to the capsular and pericapsular tissues hosted a mixed inflammatory infiltrate composed by variable proportions of small-sized lymphocytes, plasma cells, and foamy macrophages; some cases also showed multinucleated giant cells engulfing amorphous material (likely silicone). In BI-ALCL6, the inflammatory background was mainly composed by eosinophils.

Infiltration of any quantity of CD3+ and PD1+ cells was detected in all cases tested (100%): the results are summarized in Table 3. Considering the whole cohort, the median number of CD3+ TILs/HPF was 18 (mean, 56; range, 12-167); for PD1, the median number of positive TILs/HPF 7 (mean, 13; range, 1-39). The median number of TAMs expressing PDL1 per HPF was 19 (mean, 29; range, 8-83).

Most of the specimens presented a mild inflammatory infiltrate in the inner layer of the capsule; conversely, BI-ALCL2 and BI-ALCL5 showed a severe infiltrate, with >100 CD3+ TILs/HPF and >30 PD1 TILs/HPF

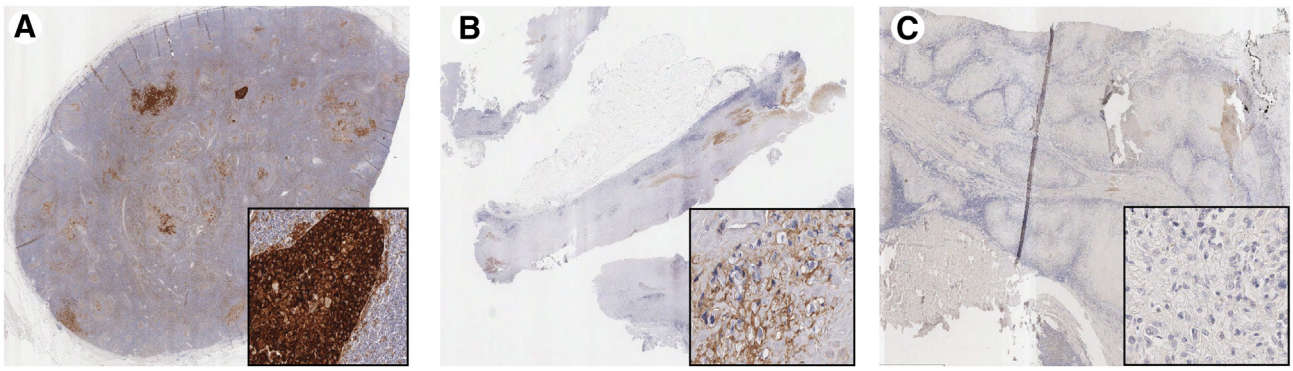

Figure 3 PDL1 immunohistochemical expression in BI-ALCLs with extracapsular disease. A, BI-ALCL 7 shows lymph node involvement with diffuse and strong PDL1 staining (H-score, 300). BI-ALCL 8 (B) and BI-ALCL 9 (C) infiltrate the capsule and the pericapsular tissues: BI-ALCL 8 is partially positive for PDL1 (H-score, 70), whereas BI-ALCL 9 is negative. Original magnification ×400.

Table 3 Quantification of PDL1-positive TAMs and of PD1+ and CD3+ TILs

Case ID	PDL1 FISH (tumor cells)	PDL1 IHC (tumor cells)	PDL1 positive TAMs/HPF [a]	PD1 positive TILs/HPF [a]	CD3 positive TILs/HPF [a]	PD1/CD3 (%)
BI-ALCL 1	Copy gain	+	10	6	18	31
BI-ALCL 2	Polysomy	+	36	18	102	18
BI-ALCL 3	Polysomy	+	20	8	12	68
BI-ALCL 4	Disomy	–	18	7	19	35
BI-ALCL 5	Disomy	–	83	39	167	23
BI-ALCL 6	Disomy	–	8	1	18	3

Abbreviation: HPF, high-power field (40×/0.75 objective lens); IHC, immunohistochemistry.
[a] HPF area equals to 0.237 mm^2.

(Table 3, Fig. 4A-D and E-H). Even if our cohort was too small to allow for a statistical comparison, PDL1-positive and PDL1-negative BI-ALCLs displayed similar values for CD3 (median, 18 versus 19 TILs/HPF), PD1 (median, 6 versus 7 TILs/HPF), and PDL1+ TAMs (median, 20 versus 18/HPF), whereas PD1/CD3 ratio was higher in PDL1-positive BI-ALCLs (median, 31% versus 23%). In particular, BI-ALCL3 hosted a very mild inflammatory infiltrate but exhibited the highest PD1/CD3 ratio (68%; Fig. 4I-L). Among PDL1-negative BI-ALCLs, we observed the highest amount of PD1+ TILs in BI-ALCL5 (39/HPF), which also presented the highest number of PDL1+ TAMs (83/HPF; Fig. 4E-H).

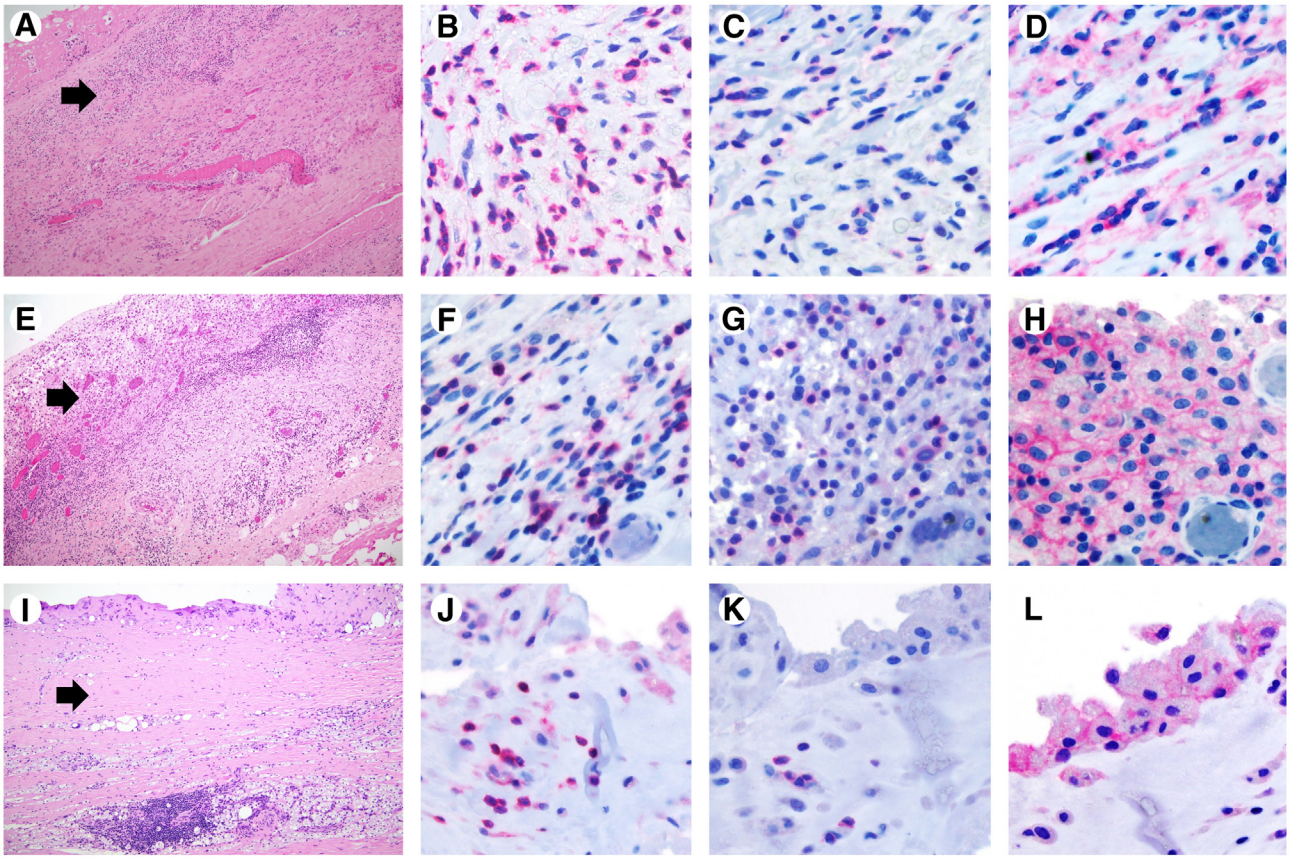

Figure 4 Analyses of PD1 and CD3 expression in TILs and PDL1 expression in TAMs. Low-power hematoxylin and eosin stain from PDL1-positive BI-ALCL 2 (A) and PDL1-negative BI-ALCL 5 (E) showing a severe inflammatory infiltrate along the inner layer of the capsule (arrows; original magnification ×100). Both samples present numerous CD3+ (B and F) and PD1+ (C and G) TILs and abundant PDL1+ TAMs (D and H). PDL1-positive BI-ALCL 3 (I) hosts a very mild inflammatory infiltrate (arrow; hematoxylin and eosin stain, original magnification ×100) but displays a high PD1/CD3 ratio because most CD3+ TILs (J) are also PD1+ (K); in addition, numerous TAMs express PDL1 (L). All immunohistochemical images were captured at an original magnification of ×400.

4. Discussion

We documented frequent PDL1 expression in BI-ALCLs, along with recurrent *PDL1* CNAs. In classical Hodgkin lymphoma, PDL1 overexpression largely correlates with *PDL1* CNAs at 9p24.1 locus [21,23]; systemic ALCLs frequently express PDL1 by immunohistochemistry, but in this type of lymphoma, *PDL1* CNAs are less common [16,19,24,25], and PDL1 overexpression is transcriptionally induced by phosphorylated STAT3 [15,16]. Enhanced expression of PDL1 on tumor cells favors immune evasion inducing functional exhaustion in tumor-infiltrating T cells through PD1 engagement [17].

PDL1 positivity has been recently reported in 3 BI-ALCL cases [18,19], but the prevalence and the genetic basis of PDL1 expression in this disease are unknown. We assessed PDL1 and pSTAT3 expression by immunohistochemistry and *PDL1* gene alterations in a cohort of 9 BI-ALCLs; we also investigated PD1/PDL1 interaction quantifying PD1+ TILs and PDL1+ TAMs in tumor microenvironment.

In keeping with previous reports [3,5,7], immunohistochemistry for pSTAT3 was consistently positive in all BI-ALCLs tested, furtherly supporting the hypothesis of a constitutive activation of the JAK/STAT3 pathway in this disease. We observed PDL1 expression in more than one-half (57%) of our cases; in particular, 2 of 3 BI-ALCLs with extracapsular involvement (67%) were positive for PDL1 staining.

Three PDL1-positive cases showed 9p24.1 CNAs: 1 case harbored PDL1 copy gain, and 2 cases were polysomic for chromosome 9. All cases with *PDL1* CNAs also showed PDL1 expression, suggesting that *PDL1* genetic alterations represent an important driver of PDL1 expression. The 9p24.1 region also harbors the Janus kinase 2 (*JAK2*) locus: 9p24.1 copy number–positive variations increase the gene dosage of both *PDL1* and its inducer, *JAK2*, that further stimulates *PDL1* transcription via JAK/STAT activity and STAT3 phosphorylation [23]. In BI-ALCL cases carrying chromosome 9 polysomy, the co-increase of JAK2 transcript abundance may have further enhanced PDL1 expression in synergy with simple *PDL1* gene-dosage effect.

However, PDL1 positivity was also observed in disomic cases, implying that constitutive JAK/STAT activation and/or other genetic pathways can also enhance PDL1 expression in the absence of increased *PDL1* gene-dosage.

It has been postulated that chronic antigen stimulation can drive BI-ALCL development by triggering T-cell activation and eventually leading to their clonal expansion in an immune tolerant milieu. In vitro studies showed that BI-ALCL cell lines can release immunosuppressive cytokines—such as IL-6, tumor growth factor band, and IL-10—that promote tumor survival and proliferation [13,14]. We found variable amounts of PD1+ TILs and PDL1+ TAMs in the inner layer of the capsule of both PDL1-positive and PDL1-negative cases. High numbers of PDL1+ TAMs may be responsible of PD1+ T-cell engagement in PDL1-negative BI-ALCLs and additionally trigger PD1/PDL1 axis in PDL1-positive BI-ALCLs. Our data furtherly uphold earlier findings that supported the role of immune escape in BI-ALCL oncogenesis: an active PDL1/PD1 axis may cooperate with the release of immunosuppressive cytokines to foster an immune-tolerant microenvironment; PDL1/PD1 ligation can shut down T-cell receptor signaling and T-cell activation, inducing an exhausted functional state in tumor-infiltrating T cells.

5. Conclusions

In summary, we identified frequent PDL1 expression and recurrent *PDL1* CNAs in BI-ALCL. Even if the small size of our series limited the statistical power of our, PD1/PDL1 axis seems to be a promising therapeutic target in BI-ALCL. Although most BI-ALCLs are successfully treated with capsulectomy alone, the subset of cases with extracapsular involvement and aggressive behavior requires a more extensive therapeutic approach; in our series, advanced-stage BI-ALCLs frequently express PDL1, suggesting the usefulness of immune-checkpoint inhibitors in these patients.

Acknowledgments

Editing. Stefano A. Pileri: Investigation, Supervision, Writing – Review & Editing.;We gratefully acknowledge Professor Umberto Gianelli for providing study materials and Virginia Maltoni, Sebastiano Spagnolo, and Pierluigi Antoniotti for their skilled technical assistance.

Supplementary data

Supplementary data to this article can be found online at https://doi.org/10.1016/j.humpath.2019.05.007.

References

[1] Feldman AL, Harris NL, Stein H, et al. Breast implant–associated anaplastic large cell lymphoma. In: Swerdlow SH, Campo E, Harris NL, et al, editors. WHO Classification of Tumours of Haematopoietic and Lymphoid Tissues. Revised 4th ed. Lyon, France: International Agency for Research on Cancer; 2017. p. 421-2.

[2] Clemens MW, Medeiros LJ, Butler CE, et al. Complete surgical excision is essential for the management of patients with breast implant–associated anaplastic large-cell lymphoma. J Clin Oncol 2016;34:160-8. https://doi.org/10.1200/JCO.2015.63.3412.

[3] Laurent C, Delas A, Gaulard P, et al. Breast implant–associated anaplastic large cell lymphoma: two distinct clinicopathological variants with different outcomes. Ann Oncol 2016;27:306-14. https://doi.org/10.1093/annonc/mdv575.

[4] Brody GS, Deapen D, Taylor CR, et al. Anaplastic large cell lymphoma occurring in women with breast implants: analysis of 173 cases. Plast Reconstr Surg 2015;135:695-705. https://doi.org/10.1097/PRS.0000000000001033.

[5] Oishi N, Brody GS, Ketterling RP, et al. Genetic subtyping of breast implant associated anaplastic large cell lymphoma. Blood 2018;132:544-7. https://doi.org/10.1182/blood-2017-12-821868.

[6] Crescenzo R, Abate F, Lasorsa E, et al. Convergent mutations and kinase fusions lead to oncogenic STAT3 activation in anaplastic large cell lymphoma. Cancer Cell 2015;27:516-32. https://doi.org/10.1016/j.ccell.2015.03.006.

[7] Blombery P, Thompson ER, Jones K, et al. Whole exome sequencing reveals activating JAK1 and STAT3 mutations in breast implant–associated anaplastic large cell lymphoma anaplastic large cell lymphoma. Haematologica 2016;101:e387-90. https://doi.org/10.3324/haematol.2016.146118.

[8] Di Napoli A, Jain P, Duranti E, et al. Targeted next generation sequencing of breast implant–associated anaplastic large cell lymphoma reveals mutations in JAK/STAT signaling pathway genes. TP53 and DNMT3A [letter Br J Haematol 2018;80:741-4. https://doi.org/10.1111/bjh.14431.

[9] Blombery P, Thompson E, Ryland GL, et al. Frequent activating STAT3 mutations and novel recurrent genomic abnormalities detected in breast implant–associated anaplastic large cell lymphoma. Oncotarget 2018;9:36126-36. https://doi.org/10.18632/oncotarget.26308.

[10] Letourneau A, Maerevoet M, Milowich D, et al. Dual JAK1 and STAT3 mutations in a breast implant–associated anaplastic large cell lymphoma. Virchows Arch 2018;473:505-11. https://doi.org/10.1007/s00428-018-2352-y.

[11] Bizjak M, Selmi C, Praprotnik S, et al. Silicone implants and lymphoma: the role of inflammation. J Autoimmun 2015;65:64-73. https://doi.org/10.1016/j.jaut.2015.08.009.

[12] Hu H, Jacombs A, Vickery K, et al. Chronic biofilm infection in breast implants is associated with an increased T-cell lymphocytic infiltrate: implications for breast implant–associated lymphoma. Plast Reconstr Surg 2015;135:319-29. https://doi.org/10.1097/PRS.0000000000000886.

[13] Lechner MG, Lade S, Liebertz DJ, et al. Breast implant–associated, ALK-negative, T-cell, anaplastic, large-cell lymphoma: establishment and characterization of a model cell line (TLBR-1) for this newly emerging clinical entity. Cancer 2011;117:1478-89. https://doi.org/10.1002/cncr.25654.

[14] Lechner MG, Megiel C`, Church CH, et al. Survival signals and targets for therapy in breast implant–associated ALK-anaplastic large cell lymphoma. Clin Cancer Res 2012;18:4549-59. https://doi.org/10.1158/1078-0432.CCR-12-0101.

[15] Marzec M, Zhang Q, Goradia A, et al. Oncogenic kinase NPM/ALK induces through STAT3 expression of immunosuppressive protein CD274 (PD-L1, B7-H1). Proc Natl Acad Sci U S A 2008;105:20852-7. https://doi.org/10.1073/pnas.0810958105.

[16] Atsaves V, Tsesmetzis N, Chioureas D, et al. PD-L1 is commonly expressed and transcriptionally regulated by STAT3 and MYC in ALK-negative anaplastic large-cell lymphoma [letter]. Leukemia 2017;31:1633-7. https://doi.org/10.1038/leu.2017.103.

[17] Dong H, Strome SE, Salomao DR, et al. Tumor associated B7-H1 promotes T-cell apoptosis: a potential mechanism of immune evasion. Nat Med 2002;8:793-800. https://doi.org/10.1038/nm730.

[18] Bianchi A, Ferrari S, Gullotta G, Grasso A, Annibali O. PD-1/PD-L1 checkpoint in breast implant–associated anaplastic large cell lymphoma: a case report. Biomed J Sci & Tech Res 2018;3(2). https://doi.org/10.26717/BJSTR.2018.03.000865.

[19] Gerbe A, Alame M, Dereure O, et al. Systemic, primary cutaneous, and breast implant–associated ALK-negative anaplastic large-cell lymphomas present similar biologic features despite distinct clinical behavior. Virchows arch; 2019. https://doi.org/10.1007/s00428-019-02570-4 Epub ahead of print.

[20] Khoury JD, Medeiros LJ, Rassidakis GZ, et al. Differential expression and clinical significance of tyrosine-phosphorylated STAT3 in ALK+ and ALK- anaplastic large cell lymphoma. Clin Cancer Res 2003;9:3692-9.

[21] Roemer MG, Advani RH, Ligon AH, et al. PDL1 and PD-L2 genetic alterations define classical Hodgkin lymphoma and predict outcome. J Clin Oncol 2016;34:2690-7. https://doi.org/10.1200/JCO.2016.66.4482.

[22] Orecchioni S, Reggiani F, Talarico G, et al. The biguanides metformin and phenformin inhibit angiogenesis, local and metastatic growth of breast cancer by targeting both neoplastic and microenvironment cells. Int J Cancer 2015;136:E534-44. https://doi.org/10.1002/ijc.29193.

[23] Green MR, Monti S, Rodig SJ, et al. Integrative analysis reveals selective 9p24.1 amplification, increased PD-1 ligand expression, and further induction via JAK2 in nodular sclerosing Hodgkin lymphoma and primary mediastinal large B-cell lymphoma. Blood 2010;116:3268-77. https://doi.org/10.1182/blood-2010-05-282780.

[24] Luchtel RA, Dasari S, Oishi N, et al. Molecular profiling reveals immunogenic cues in anaplastic large cell lymphomas with DUSP22 rearrangements. Blood 2018;132:1386-98. https://doi.org/10.1182/blood-2018-03-838524.

[25] Panjwani PK, Charu V, DeLisser M, Molina-Kirsch H, Natkunam Y, Zhao S. Programmed death-1 ligands PD-L1 and PD-L2 show distinctive and restricted patterns of expression in lymphoma subtypes. Hum Pathol 2018;71:91-9. https://doi.org/10.1016/j.humpath.2017.10.029.